J|A|C|S ARTICLES

Published on Web 09/22/2009

Redox-Active Metallomacrocycles and Cyclic Metallopolymers: Photocontrolled Ring-Opening Oligomerization and Polymerization of Silicon-Bridged [1]Ferrocenophanes Using Substitutionally-Labile Lewis Bases as Initiators

David E. Herbert,[†] Joe B. Gilroy,[†] Wing Yan Chan,[‡] Laurent Chabanne,[†] Anne Staubitz,[†] Alan J. Lough,[§] and Ian Manners*,[†]

School of Chemistry, University of Bristol, Cantock's Close, Bristol, England, BS8 1TS
Department of Chemistry, X-ray Crystallography, University of Toronto, 80 St. George Street, Toronto, Ontario, Canada, M5S 3H6

Received June 22, 2009; E-mail: ian.manners@bristol.ac.uk

Abstract: Irradiation of silicon-bridged [1]ferrocenophane [Fe(η-C_5H_4)$_2$SiMe$_2$] (**1**) in the presence of substitutionally labile Lewis bases such as 4,4′-dimethyl-2,2′-bipyridine (Me_2bpy) initiates ring-opening polymerization and oligomerization via cleavage of an iron−cyclopentadienyl bond. A distribution of cyclic polyferrocenylsilane **c-PFS** (PFS = [Fe(η-C_5H_4)$_2$SiMe$_2$]$_n$) and a series of cyclic oligomers (**2$_2$**−**2$_7$**) were isolated by column chromatography and fully characterized. Varying temperature and concentration were found to influence the molecular weight distribution and the ratio of polymer to oligomer products, enabling the formation of **c-PFS** with molecular weights >100 kDa. Cyclic polymer samples were found to possess lower hydrodynamic radii and viscosity and higher glass transition temperatures than those of their linear PFS counterparts (**l-PFS**) of comparable molecular weight. Compared with crystalline samples of **l-PFS** of similar molecular weights, **c-PFS** formed smaller spherulites, as observed by polarizing optical microscopy. While the wide-angle X-ray scattering (WAXS) patterns from lower molecular weight **l-PFS** were found to differ from those from higher molecular weight samples, those obtained for lower and higher molecular weight samples of **c-PFS** are identical and resemble diffraction patterns of high molecular weight **l-PFS**. The electrochemical behavior of each cyclic oligomer **2$_2$**−**2$_7$** was studied by cyclic and differential pulse voltammetry and was found to depend on whether the oligomer contains an odd or even number of ferrocene units. In contrast to linear analogs, two reversible redox processes of varying intensities were observed for cyclic oligomers containing an even number of iron centers, while three reversible redox processes of varying intensities were observed for cyclic oligomers containing an odd number of iron centers. As the oligomer chain length increased, the electrochemical behavior of all cyclic oligomers approached that of both cyclic and linear high molecular weight polymers.

1. Introduction

Cyclic polymers exhibit interesting and important differences in their physical and chemical behavior compared to their linear counterparts.[1,2] For example, the ring topology of cyclic macromolecules can persist in isolated objects or in self-assembled systems and has been observed in the solid-state.[3] In addition, cyclic polymers are ideal test materials for examining the role of chain ends in the behavior of long chain polymers, such as in the hypothesis that reptation is the sole mechanism for polymer mobility.[4] Recent reports developing the catalytic production of high molecular weight cyclic polyethylene

[†] University of Bristol.
[‡] Department of Chemistry, University of Toronto.
[§] X-ray Crystallography, University of Toronto.

(1) (a) Semlyen, J. A., Ed. *Cyclic Polymers*, 2nd ed.; Academic Publishers: Dordrecht, Netherlands, 2000. (b) Hadjichristidis, N.; Pitsikalis, M.; Pispas, S.; Iatrou, H. *Chem. Rev.* **2001**, *101*, 3747. (c) Oike, H. *Reactive & Functional Polymers* **2007**, *67*, 1157. (d) Feng, W.; Yamato, K.; Yang, L.; Ferguson, J. S.; Zhong, L.; Zou, S.; Yuan, L.; Zeng, X. C.; Gong, B. *J. Am. Chem. Soc.* **2009**, *131*, 2629.
(2) Deffieux, A.; Borsali, R. *Macromol. Eng.* **2007**, *2*, 875.
(3) (a) Schappacher, M.; Deffieux, A. *J. Am. Chem. Soc.* **2008**, *130*, 14684. (b) Schappacher, M.; Deffieux, A. *Science* **2008**, *319*, 1512. (c) Chou, T.-F.; So, C.; White, B. R.; Carlson, J. C. T.; Sarikaya, M.; Wagner, C. R. *ACS Nano* **2008**, *2*, 2519.
(4) McLeish, T. *Science* **2002**, *297*, 2005.
(5) (a) Bielawski, C. W.; Benitez, D.; Grubbs, R. H. *Science* **2002**, *297*, 2041. (b) Boydston, A. J.; Xia, Y.; Kornfield, J. A.; Gorodetskaya, I. A.; Grubbs, R. H. *J. Am. Chem. Soc.* **2008**, *130*, 12775.
(6) Xia, Y.; Boydston, A. J.; Yao, Y.; Kornfield, J. A.; Gorodetskaya, I. A.; Spiess, H. W.; Grubbs, R. H. *J. Am. Chem. Soc.* **2009**, *131*, 2670.
(7) Known metallomacrocycles are often prepared by metal-mediated self-assembly and stabilized through noncovalent interactions. For recent reviews, see: (a) Leininger, S.; Olenyuk, B.; Stang, P. J. *Chem. Rev.* **2000**, *100*, 853. (b) Zangrando, E.; Casanova, M.; Alessio, E. *Chem. Rev.* **2008**, *108*, 4979.
(8) (a) Tamm, M.; Kunst, A.; Herdtweck, E. *Chem. Commun.* **2005**, 1729. (b) We have previously reported evidence that low molecular weight **c-PFS** (M_n < 4700) is formed from the very slow (1.5 day) reaction of **1** with a platinasila[2]ferrocenophane catalyst in the presence of BH_3·THF. See: Temple, K.; Lough, A. J.; Sheridan, J. B.; Manners, I. *J. Chem. Soc., Dalton Trans.* **1998**, 2799.

 10.1021/ja904928c CCC: $40.75

highlight some of the advances made in cyclic organic polymer synthesis.[5,6] In comparison to the progress with organic systems, main group and metallomacrocycles,[7,8] aside from cyclic polysilanes[9] and polysiloxanes,[10] are virtually unexplored.

Polymers containing transition metals in the main chain have shown utility as multifunctional materials in a variety of applications.[11,12] Linear polyferrocenylsilanes (**l-PFSs**) represent one of the most widely studied metallopolymer systems.[13] Silicon-bridged [1]ferrocenophanes (sila[1]ferrocenophanes) such as **1** possess substantial ring strain, and the ability of these and related metal-containing rings to undergo ring-opening polymerization (ROP) to give linear homo- and block copolymers has been well-studied.[14] Cyclic analogues of **l-PFSs** are much less explored. The smallest of these species, disila[1.1]ferrocenophane (**2$_2$**),[15−18] and many other cyclic ferrocene dimers with a wide variety of bridging elements comprise the bulk of known compounds.[19] As the number of ferrocene units increases, cyclic oligomers are increasingly more difficult to prepare, and there exist only a handful of literature reports of their synthesis.[20] The largest, a cycle of seven ferrocene units (**3**), was prepared in 1997 in 6% yield by Köhler and co-workers and was also the largest cyclic ferrocene oligomer known at the time.[21]

We have recently developed a photocontrolled, living anionic ring-opening polymerization route to **l-PFSs**. These reactions proceed through photoinduced cleavage of an iron−cyclopentadienyl (Fe−Cp) bond in monomers such as **1**, which can be initiated by [C_5H_5]$^-$ (Cp$^-$) anions to provide a novel, controlled means to prepare new linear PFS homo- and block copolymers.[22−24] When 1,2-bis(diphenylphosphino)ethane (DPPE) was used in place of the Na[C_5H_5] initiator at 5 °C, irradiation afforded the ring-slipped species **4** as the sole product and no polymer was detected.[25,26] To investigate the generality of this unusual chemistry, we have examined reactions in the presence of other heteroatom-containing bidentate ligands with the aim of producing structural analogues to **4**. In a recent preliminary report,[27] we showed that the photocontrolled ring opening of **1** produces cyclic PFS (**c-PFS**) in high yield when initiated by neutral Lewis donors (e.g., 4,4′-dimethyl-2,2′-bipyridine). We herein present full details of the isolation and characterization of **c-PFS** and a range of cyclic oligomers, the [1^n]ferrocenophanes **2$_x$** ($x = 2-7$) and compare their properties with those of the corresponding linear materials.

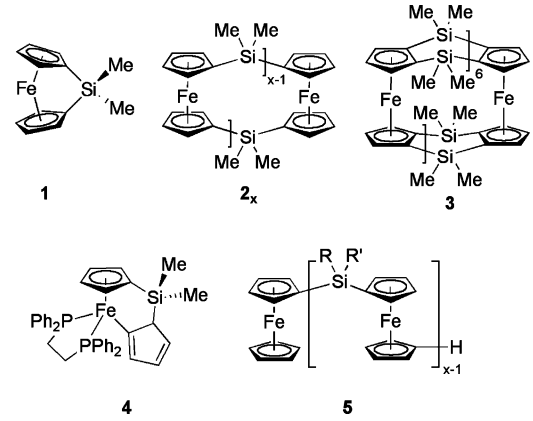

2. Results and Discussion

2.1. Synthesis, Isolation, and Characterization of Cyclic PFS (c-PFS) and the Cyclic Oligo(ferrocenylsilanes) 2$_{2-7}$. Irradiation of **1** (Hg lamp, Pyrex glassware: $\lambda > 310$ nm) in the presence of a stoichiometric quantity of 4,4′-dimethyl-2,2′-bipyridine (Me_2bpy) for 2 h at 35 °C in THF caused a color change in the solution from red to orange-brown. Analysis of the reaction mixture by ^{1}H NMR spectroscopy showed the complete conversion of ferrocenophane **1** into multiple products, including a polymeric fraction (35%) and the known cyclic

(9) Zirngast, M.; Baumgartner, J.; Marschner, C. *Organometallics* **2008**, *27*, 6472.
(10) (a) Arrighi, V.; Gagliardi, S.; Dagger, A. C.; Semlyen, J. A.; Higgins, J. S.; Shenton, M. J. *Macromolecules* **2004**, *37*, 8057. (b) Clarson, S. J. *Cyclic Polymers (2nd Edition)* **2000**, 161. (c) Gagliardi, S.; Arrighi, V.; Ferguson, R.; Dagger, A. C.; Semlyen, J. A.; Higgins, J. S. *J. Chem. Phys.* **2005**, *122*, 064904/1. (d) Liu, L.-M.; Zhang, B.-Y.; He, X.-Z.; Cheng, C.-S. *Liq. Cryst.* **2004**, *31*, 781.
(11) (a) Newkome, G. R.; He, E.; Moorefield, C. N. *Chem. Rev.* **1999**, *99*, 1689. (b) Manners, I. *Synthetic Metal-Containing Polymers*; Wiley-VCH: Weinheim, 2004. (c) Holliday, B. J.; Swager, T. M. *Chem. Commun.* **2005**, 23. (d) Korczagin, I.; Lammertink, R. G. H.; Hempenius, M. A.; Golze, S.; Vancso, G. J. *Adv. Polym. Sci.* **2006**, *200*, 91. (e) Williams, K. A.; Boydston, A. J.; Bielawski, C. W. *Chem. Soc. Rev.* **2007**, *36*, 729.
(12) (a) Whittell, G. R.; Manners, I. *Adv. Mater.* **2007**, *19*, 3439. (b) Astruc, D.; Ornelas, C.; Ruiz, J. *Acc. Chem. Res.* **2008**, *41*, 841.
(13) (a) Foucher, D. A.; Tang, B. Z.; Manners, I. *J. Am. Chem. Soc.* **1992**, *114*, 6246. (b) Manners, I. *Chem. Commun.* **1999**, 857. (c) Bellas, V.; Rehahn, M. *Angew. Chem. Int. Ed.* **2007**, *46*, 5082.
(14) Herbert, D. E.; Mayer, U. F. J.; Manners, I. *Angew. Chem. Int. Ed.* **2007**, *46*, 5060.
(15) Ni, Y.; Rulkens, R.; Pudelski, J. K.; Manners, I. *Macromol. Rapid Commun.* **1995**, *16*, 637.
(16) Park, J.; Seo, Y.; Cho, S.; Whang, D.; Kim, K.; Chang, T. *J. Organomet. Chem.* **1995**, *489*, 23.
(17) Zechel, D. L.; Foucher, D. A.; Pudelski, J. K.; Yap, G. P. A.; Rheingold, A. L.; Manners, I. *J. Chem. Soc., Dalton Trans.* **1995**, 1893.
(18) (a) Calleja, G.; Carré, F.; Cerveau, G.; Labbé, P.; Coche-Guérente, L. *Organometallics* **2001**, *20*, 4211. (b) Berenbaum, A.; Lough, A. J.; Manners, I. *Organometallics* **2002**, *21*, 4415.
(19) (a) Brunner, H.; Klankermayer, J.; Zabel, M. *J. Organomet. Chem.* **2000**, *601*, 211. (b) Uhl, W.; Hahn, I.; Jantschak, A.; Spies, T. *J. Organomet. Chem.* **2001**, *637−639*, 300. (c) Althoff, A.; Jutzi, P.; Lenze, N.; Neumann, B.; Stammler, A.; Stammler, H.-G. *Organometallics* **2002**, *21*, 3018. (d) Scheibitz, M.; Winter, R. F.; Bolte, M.; Lerner, H.-W.; Wagner, M. *Angew. Chem. Int. Ed.* **2003**, *42*, 924. (e) Braunschweig, H.; Burschka, C.; Clentsmith, G. K. B.; Kupfer, T.; Radacki, K. *Inorg. Chem.* **2005**, *44*, 4906. (f) Schachner, J. A.; Orlowski, G. A.; Quail, J. W.; Kraatz, H.-B.; Mueller, J. *Inorg. Chem.* **2006**, *45*, 454. (g) Ieong, N. S.; Chan, W. Y.; Lough, A. J.; Haddow, M. F.; Manners, I. *Chem.−Eur. J.* **2008**, *14*, 1253.
(20) (a) Lippard, S. J.; Martin, G. *J. Am. Chem. Soc.* **1970**, *92*, 7291. (b) Mueller-Westerhoff, U. T. *Angew. Chem. Int. Ed.* **1986**, *25*, 702. (c) Mueller-Westerhoff, U. T.; Swiegers, G. F. *Chem. Lett.* **1994**, 67. (d) Mizuta, T.; Aotani, T.; Imamura, Y.; Kubo, K.; Miyoshi, K. *Organometallics* **2008**, *27*, 2457.
(21) Grossmann, B.; Heinze, J.; Herdtweck, E.; Köhler, F. H.; Nöth, H.; Schwenk, H.; Spiegler, M.; Wachter, W.; Weber, B. *Angew. Chem. Int. Ed.* **1997**, *36*, 387.
(22) Tanabe, M.; Manners, I. *J. Am. Chem. Soc.* **2004**, *126*, 11434.
(23) Tanabe, M.; Vandermeulen, G. W. M.; Chan, W. Y.; Cyr, P. W.; Vanderark, L.; Rider, D. A.; Manners, I. *Nat. Mater.* **2006**, *5*, 467.
(24) For work on Fe−Cp bond cleavage reactions in phosphorus-bridged [1]ferrocenophanes and the isolation of cyclic dimers and trimers, see: (a) Mizuta, T.; Imamura, Y.; Miyoshi, K. *J. Am. Chem. Soc.* **2003**, *125*, 2068. (b) Mizuta, T.; Imamura, Y.; Miyoshi, K.; Yorimitsu, H.; Oshima, K. *Organometallics* **2005**, *24*, 990. (c) Imamura, Y.; Kubo, K.; Mizuta, T.; Miyoshi, K. *Organometallics* **2006**, *25*, 2301.
(25) Tanabe, M.; Bourke, S. C.; Herbert, D. E.; Lough, A. J.; Manners, I. *Angew. Chem. Int. Ed.* **2005**, *44*, 5886.
(26) Herbert, D. E.; Tanabe, M.; Bourke, S. C.; Lough, A. J.; Manners, I. *J. Am. Chem. Soc.* **2008**, *130*, 4166.
(27) Preliminary communication: Chan, W. Y.; Lough, A. J.; Manners, I. *Angew. Chem. Int. Ed.* **2007**, *46*, 9069.

Scheme 1. Mechanism for Ring-Expansion Macrocyclization of **1**[a]

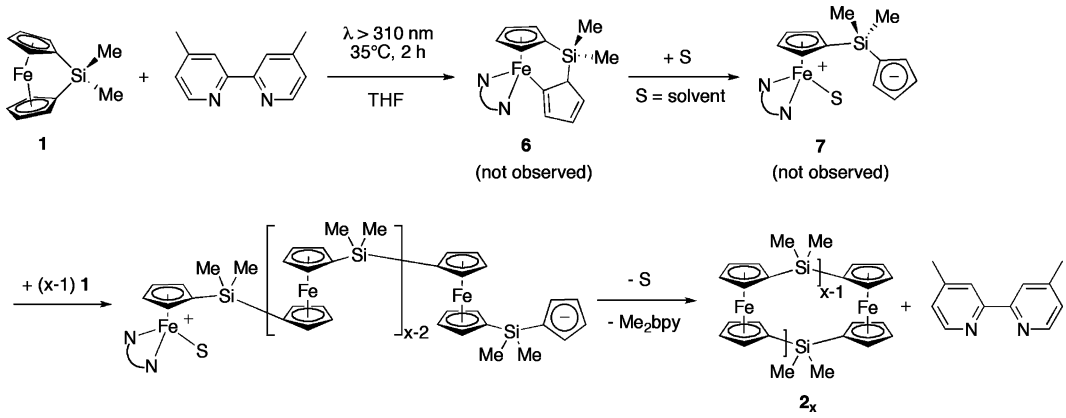

[a] A backbiting mechanism would account for small values of x; macrocondensation of two or more chains would lead to larger values of x.

dimer $\mathbf{2_2}$ (20%). The identification of the cyclic dimer in the reaction mixture prompted us to search for other oligo(ferrocenyldimethylsilanes). These were separated from higher molecular weight polymer by extraction into hexanes, in which the polymer is insoluble. The hexanes extract was found to contain a distribution of oligomers ($x < 8$). The cyclic dimer $\mathbf{2_2}$, trimer $\mathbf{2_3}$, tetramer $\mathbf{2_4}$, pentamer $\mathbf{2_5}$, hexamer $\mathbf{2_6}$, and heptamer $\mathbf{2_7}$ were separated by column chromatography and identified by MALDI-TOF mass spectrometry. Oligomers $\mathbf{2_{3-7}}$ are rare examples of cyclic ferrocenes containing more than two ferrocene units; they are also analogues of linear oligoferrocenylsilanes ($\mathbf{5_{2-9}}$) we and others have previously synthesized by the lithioferrocene-initiated anionic oligomerization of sila[1]-ferrocenophane **1**.[28−30]

Scheme 1 illustrates a proposed mechanism for the formation of cyclic ferrocenyldimethylsilane oligomers and polymers from the irradiation of **1** in the presence of a stoichiometric amount of Me_2bpy. The formation of polymeric products in this reaction indicated that chain propagation (i.e., the reaction of a pendant Cp^- chain end with **1** or **6**) is rapid. By analogy with the isolable dppe derivative **4**, initial photoinduced Me_2bpy coordination and Cp ring slippage are thought to generate a species with the proposed structure of **6** (not observed). The η^1-coordinated Cp ring may then dissociate from the iron center (**7**, not observed) with the possible addition of a molecule of solvent. The freed, pendant Cp anion can then induce rapid chain propagation upon reaction with further equivalents of **1** or **6** to yield a growing polymer chain.

The $[P_nCpFe(Me_2bpy)S]^+$ (P_n = polymer chain, S = solvent, e.g., THF) end group of the PFS macromolecule is likely to be highly reactive, and so the pendant Cp anion at the other end of the polymer chain may then "backbite" to close the polymer ring. We have previously demonstrated that the heteroleptic cationic complex $[(Me_3P)_3Fe\{(\eta^5\text{-}C_5H_4)CH_2CH_2(C_5H_5)\}]^+$ will react with free $[C_5H_5]^-$ anions to form metallocene derivatives with concomitant loss of 3 equiv of PMe_3 but only with irradiation (λ > 310 nm).[26] A similar process here (with or without irradiation) would release Me_2bpy and yield cyclic oligo(ferrocenyldimethylsilanes) with a distribution of ring sizes ($\mathbf{2_x}$, $x \geq 2$). Compared to the photolysis of **1** in the presence of dppe, the propensity for backbiting during chain growth in the Me_2bpy reaction is presumably a consequence of the weaker binding strength of Me_2bpy at the soft Fe^{II} center. Macrocondensation of two or more growing chains would potentially compete with ring closure, leading to higher values of x and increasing the breadth of the molecular weight distribution.

Table 1. Photopolymerization of **1** (Me_2bpy Initiator) in THF (2 h Irradiation)

run	T (°C)	[1]/M	**c-PFS** (%)[a]	$\mathbf{2_{2-7}}$ (%)[a]	M_n[b]	PDI[b]	MALDI-TOF[c]
1	−10	0.21	65	35	30 300	1.8	3876 (16)
2	−5	0.21	70	19	30 800	1.6	4118 (17)
3	15	0.21	54	44	24 600	1.7	4601 (19)
4	15	0.10	62	38	32 900	1.7	6056 (25)
5	25	0.21	51	47	24 600	1.7	4846 (20)
6	25	0.10	23	77	17 100	1.8	4847 (20)
7	35	0.21	39	50	20 900	1.5	5329 (22)
8	35	0.10	24	47	11 900	2.1	7751 (32)
9	35[d]	0.14	55	45	21 600	1.8	4846 (20)
10	55	0.21	8	9	3800	1.5	2441 (10)

[a] % yield **c-PFS** $\mathbf{2_x}$ ($x \geq 8$) and cyclic oligomers $\mathbf{2_{2-7}}$ calculated from methyl signal integrals in the ^1H NMR spectrum of the reaction mixture. [b] Of **c-PFS** $\mathbf{2_x}$ ($x \geq 8$) separated from oligomers by precipitation into hexanes estimated by GPC (conventional calibration). [c] Central peak of observed distribution for **c-PFS** (number of repeat units). Under our experimental conditions, only low molecular weight fractions ionized. [d] 4 h irradiation.

Increasing the initial concentration of **1** increased the number-average molecular weight of **c-PFS** (see Table 1). Significantly, lower temperatures, extended irradiation times, and increased initial concentrations of **1** decreased the amount of unreacted monomer. Performing the irradiation of **1** and Me_2bpy in THF for 2 h at lower temperatures (down to −10 °C) increased both the yield and molecular weight of **c-PFS** ($\mathbf{2_x}$, $x \geq 8$) relative to cyclic oligomers ($\mathbf{2_x}$, $x < 8$). We have previously demonstrated[23] that polymerization of **1** using initiators which cleave an Fe−Cp bond does not occur at ambient or subambient temperatures in the dark, so only intermediates formed from the photoexcited monomer[31] add to the growing polymer chain. We assume that this primary photochemical intermediate must have a shorter lifetime at higher temperatures, and therefore a lower concentra-

(28) The degree of polymerization for each oligoferrocenylsilane is indicated by a subscript in its compound number. For example, $\mathbf{2_2}$ refers to the cyclic dimer disila[1.1]ferrocenophane.

(29) (a) Lough, A. J.; Manners, I.; Rulkens, R. *Acta Crystallogr., Sect. C* **1994**, *50*, 1667. (b) Pannell, K. H.; Dementiev, V. V.; Li, H.; Cervantes-Lee, F.; Nguyen, M. T.; Diaz, A. F. *Organometallics* **1994**, *13*, 3644.

(30) Rulkens, R.; Lough, A. J.; Manners, I.; Lovelace, S. R.; Grant, C.; Geiger, W. E. *J. Am. Chem. Soc.* **1996**, *118*, 12683.

(31) This photochemical intermediate likely involves ring slippage of a Cp ring, with coordination of one or more solvent molecules such as THF, in analogy to compounds such as **4**.

Table 2. Molecular Weight Data for As-Prepared Bulk Polymer Samples of **c-PFS**

run	T (°C)	isolated yield (%)	M_n[a]	M_w[a]	PDI[a]
11	−10	59	43 900	99 000	2.3
12	0	56	48 800	125 400	2.6
13	10	52	16 200	60 100	3.7
14	20	60	17 000	54 600	3.2
15	35	58	18 700	40 800	2.2
16	55	27	14 000	31 600	2.3
17[b]	55	32	31 600	66 500	1.9

[a] Calculated from GPC (triple detection). Polydispersity index (PDI) = M_w/M_n. [b] [**1**] = 0.52 M. All other reactions [**1**] = 0.26 M.

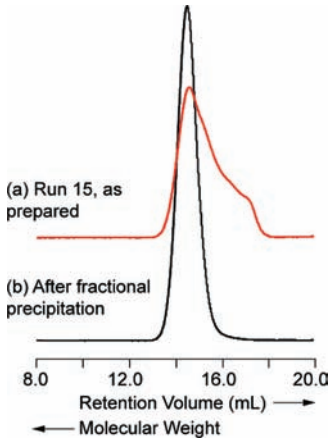

Figure 1. GPC traces of **c-PFS** (Run 15, Table 2): (a) as-prepared and (b) precipitated **c-PFS** (hexanes/THF). Molecular weight increases right to left.

Table 3. More Well-Defined **c-PFS** Samples Isolated Following Fractional Precipitation

polymer	T (°C)	M_n[a]	M_w[a]	PDI[a]
15a	35	12 800	19 100	1.5
15b	35	56 700	66 300	1.2
14a	20	80 700	107 500	1.3
12a	−5	160 000	228 600	1.4
11a	−10	182 900	221 200	1.2

[a] Calculated from GPC (triple detection). Polydispersity index (PDI) = M_w/M_n.

tion of the photoexcited monomer is present for photocontrolled polymerization, which slows the rate of propagation.[23]

Analysis of the isolated **c-PFS** by triple-detection gel permeation chromatography (GPC) gave absolute molecular weights for the polymer samples (Table 2). Broad molecular weight distributions of **c-PFS** were always observed for these samples as prepared, presumably arising from backbiting and macrocondensation reactions that disrupt chain propagation in a random fashion. Samples of **c-PFS** with narrow molecular weight distributions (M_w/M_n < 1.5) could be separated by fractional precipitation of larger molecular weight samples from THF through the addition of hexanes (Figure 1, Table 3). These more well-defined molecular weight polymer samples were used to investigate the effect of ring size on polymer properties, such as thermal transitions.

(32) It is known that the most probable molecular weights obtained by MALDI-TOF MS and GPC only show good agreement for polymers with a narrow molecular weight distribution (PDI <1.1). For polydisperse polymers, MALDI-TOF MS will show significant molecular weight discrimination. For a comprehensive discussion, see: Nielen, M. W. F. *Mass Spec. Rev.* **1999**, *18*, 309, and references therein.

To establish the cyclic nature of the products, we noted the absence of end groups in ^{1}H and ^{13}C NMR spectra of samples of **c-PFS**. In addition, we examined samples of **c-PFS** by nonfragmentary MALDI-TOF mass spectrometry to determine whether end groups could be observed for higher molecular weight samples.[32] Analysis was performed on well-mixed solutions of polymer samples (1 mg/mL) in CH_2Cl_2 or THF and a saturated THF solution of dithranol as matrix (in a 1:5 volume ratio). Cyclic oligo- and poly(ferrocenylsilanes) with upward of 32 repeat units were unambiguously confirmed not to contain end groups and the observed distributions conformed to integer multiples of the molecular weight of the repeat unit **1**. When compared with samples of **l-PFS 8** (M_n = 5120; PDI = 1.02) prepared by anionic polymerization using *n*BuLi as initiator and terminated with MeOH, the MALDI-TOF spectra of the latter showed a distinct shift corresponding to the presence of end groups (Figure 2). Samples with molecular weights much greater than ∼10 000 Da did not ionize under the experimental conditions employed.

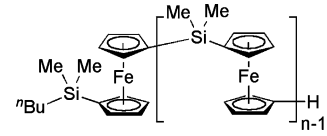

8

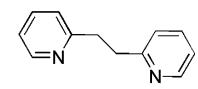

9

Consistent with their cyclic structure, **c-PFS** macromolecules are more compact in solution compared to **l-PFS**. For example, the ratio of hydrodynamic radii, $R_{h,cyclic}/R_{h,linear}$, measured for polymer **15b** (Table 3, M_w = 66 300, PDI = 1.2) and a **l-PFS** of similar molecular weight (M_w = 68 240, PDI = 1.1) is 0.88, which compares with values of 0.86−0.90 cited in the literature.[2] In addition, Mark−Houwink plots of **c-PFS** and **l-PFS** showed that the cyclic polymers have lower intrinsic viscosity than their linear counterparts of the same molecular weight as determined by triple-detection GPC (see Figure S5 in the Supporting Information).

An important issue to address for all samples of cyclic polymers is the presence of topological impurities (e.g., linear contaminants or interlinked rings).[6] Examining the GPC traces of as-prepared, bulk samples of **c-PFS**, the molecular weight distributions are quite broad and show distinct tailing into the lower molecular weight region (higher retention volume, Figure 1). The absence of tailing at the higher molecular weight end of the GPC trace is consistent with backbiting ring-closing reactions dominating over macrocondensation reactions, which would produce very high molecular weight polymer chains that would be less likely to backbite and form **c-PFS**. In conjunction with the absence of end group resonances in ^{1}H NMR spectra, this suggests that **c-PFS** samples which are too high in molar mass to be examined by MALDI-TOF MS are predominantly cyclic.

The mechanism proposed in Scheme 1, however, does not preclude the formation of linear contaminants. Indeed, in some cases where the photocontrolled reactions were performed under dilute conditions and the reaction mixtures were precipitated directly into methanol, evidence for the presence of uncyclized **l-PFS** contaminants was detected by MALDI-TOF. This situation was avoided by performing the photo-oligomerization/polymerization reactions at higher concentrations.[33] Based on our experimental results, longer reaction times and lower temperatures also minimize the amount of linear impurities.

We attribute the interesting ring-opening closing macrocyclization of **1** to the substitutional lability of the Me_2bpy ligand

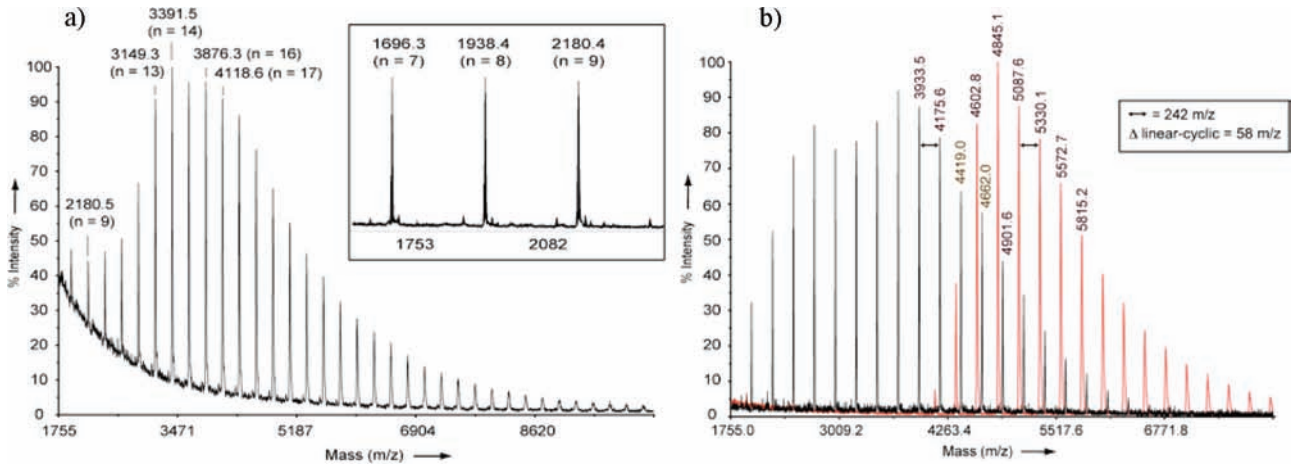

Figure 2. (a) MALDI-TOF spectrum (linear mode) of **c-PFS** (run 11). Inset: lower molecular weight fraction (reflector mode). (b) Overlay of MALDI-TOF spectra of **l-PFS 8** (black trace) and **c-PFS** (red trace).

Scheme 2. High-Yield Preparation of $\mathbf{2_2}$ from Irradiation of **1** with LiCl in THF

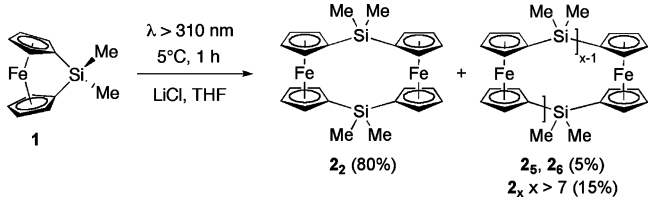

on the end group of a growing PFS chain (Scheme 1). This prompted us to explore the use of other neutral or weakly coordinating ligands to induce Cp ring slippage in [1]ferrocenophanes. With monodentate phosphines such as PMe_3 or PPh_3, only high molecular weight cyclic PFS formed and no small cyclic oligomers (e.g., $\mathbf{2}_{2-7}$) were observed.[26] Irradiation of **1** with 2,2′-bipyridine (bpy) led to **c-PFS** and smaller oligomers. Irradiation of **1** with analogues of these bipyridine initiators did not. For example, no reaction was observed between **1** and the structural isomer of Me_2bpy, 2,2′-ethane-1,2-diyldipyridine (**9**), when irradiated in THF at 35 or 5 °C. While coordination of 1 or 2 equiv of bis(1,2-dimethylphosphino)ethane (dmpe) to **1** has been observed at 5 °C, irradiation of THF solutions of **1** with chelating bidentate ethers or amines, such as bis(1,2-dimethoxy)ethane (DME) or *N*,*N*,*N*′,*N*′-tetramethylethylenediamine (TMEDA), did not show evidence of stable coordination or cyclo-oligomerization. Furthermore, neither acetonitrile nor the tridentate amine, *N*,*N*,*N*′,*N*″,*N*″-pentamethyldiethylenetriamine led to any detectable reaction when irradiated with compound **1**.

Irradiation of a THF solution of ferrocenophane **1** and LiCl (2 equiv.), however, at 5 °C for 1 h resulted in a color change from red to orange, indicating that the ferrocenophane had undergone ring-opening. Analysis of the reaction mixture by ^{1}H NMR spectroscopy showed the formation of **c-PFS** in 15% yield and the cyclic dimer $\mathbf{2_2}$ in 80% yield. Small amounts (5%) of other oligomers were also detected. This reaction (Scheme 2) is a convenient one-step preparation for cyclic dimer $\mathbf{2_2}$ in high yield, without involving a multistep synthesis (with yields of 15%[17] or 21%[16]) or metal catalysts.[15,34] A ring-slipped species with two chloride ligands coordinated to the iron atom was not observed. The formation of the cyclic dimer as the major product points to the labile nature of the chloride ligands: presumably, instead of continuously ring-opening more of ferrocenophane **1**, the propagating Cp anion predominantly backbites after a second unit of **1** is ring-opened, releasing the two chloride ligands and $\mathbf{2_2}$. Lower temperatures or higher concentrations of **1** increase the proportion of **c-PFS** relative to the cyclic dimer.

When a THF solution of ferrocenophane **1** and LiOTf (2 equivalents) was irradiated for 1 h at 5 °C, no color change was observed and ^{1}H NMR spectroscopy showed no evidence of a reaction. This was expected as triflate is a much weaker nucleophile than chloride in THF, so the former is not expected to coordinate to the iron atom of the photoexcited ferrocenophane.[31] As anticipated from the LiOTf and DME irradiation experiments, no reaction was observed following 1 h of irradiation of **1** with $LiBPh_4 \cdot 3$ DME.

2.2. Thermal Transition Behavior and Morphological Studies of c-PFS. c-PFSs, like their linear counterparts, are semicrystalline amber solids. Accordingly, differential scanning calorimetry (DSC) studies of **c-PFS** samples showed a change in heat capacity (at temperature T_g) and melting of crystallites (at temperature T_m). The equilibrium T_m of symmetrically substituted linear poly(ferrocenyldimethylsilane)s was previously determined by DSC to be 143 °C.[35,36] The onset temperature of the melt endotherms observed for **c-PFS** samples varied with annealing temperature. The equilibrium values estimated from DSC studies of **c-PFS** (154 °C) were found to be slightly higher than those for **l-PFS**. The crystallinity of **c-PFS** is further discussed below.

In terms of the glass transition, it has been predicted[37] that the glass temperature (T_g) of low molecular weight cyclic polymers should be higher than that for corresponding linear macromolecules with the same number of repeat units. As a ring has lower configurational entropy than a linear chain, fewer degrees of freedom are involved in the glass transition. Thus,

(33) For some samples formed under dilute conditions and purified by direct precipitation of the reaction mixtures into methanol, evidence for **l-PFS** with MeO-end groups was found using MALDI-TOF MS. For details see Figure S2 and associated discussion in the Supporting Information.

(34) Reddy, N. P.; Choi, N.; Shimada, S.; Tanaka, M. *Chem. Lett.* **1996**, 649.
(35) Lammertink, R. G. H.; Hempenius, M. A.; Manners, I.; Vancso, G. J. *Macromolecules* **1998**, *31*, 795.
(36) Papkov, V. S.; Gerasimov, M. V.; Dubovik, I. I.; Sharma, S.; Dementiev, V. V.; Pannell, K. H. *Macromolecules* **2000**, *33*, 7107.
(37) Di Marzio, E. A.; Guttman, C. M. *Macromolecules* **1987**, *20*, 1403.

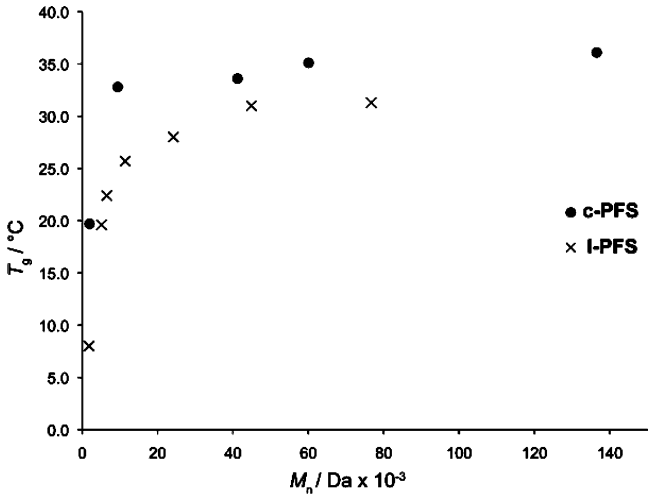

Figure 3. Glass transition temperature (T_g) as a function of M_n as measured by DSC.

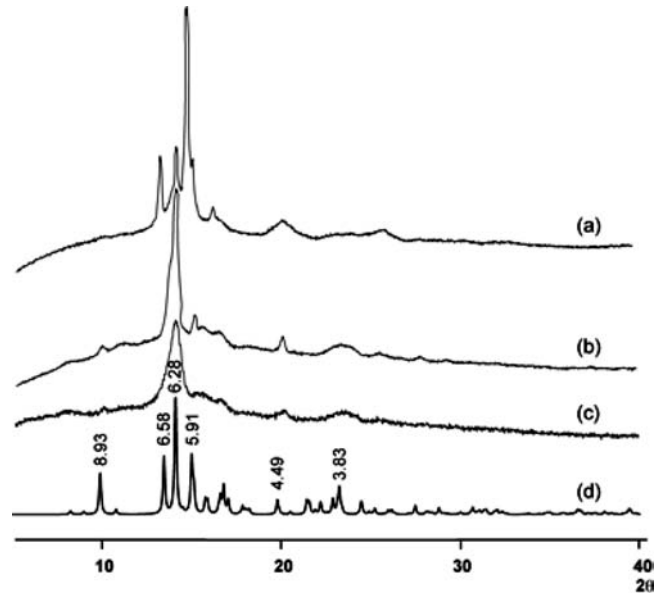

Figure 4. (a) **l-PFS**, $M_n = 5120$, PDI = 1.02; (b) **c-PFS**, $M_n = 4960$, PDI = 1.13; (c) **l-PFS**, $M_n = 62\,290$, PDI = 1.10; (d) simulated powder pattern of linear pentamer $\mathbf{5_5}$ ($\lambda = 1.542$ Å). Peaks are labeled with corresponding *d*-spacings (Å).

for cyclic polymers, T_g should increase with decreasing molecular weight. Theoretical work, however, predicts higher T_g values than those experimentally determined,[38] and it has been suggested that some models have overestimated the effect of cyclization on the T_g.[39]

In practice, a variety of behaviors have been reported. For example, cyclic poly(dimethylsiloxanes) show increasing values of T_g with decreasing molecular weight, from a limiting value of −123.1 °C ($M_n > 1730$) up to − 116.3 °C ($M_n = 500$).[38] In contrast, T_g values for cyclic polystyrene (c-PS) and cyclic poly(2-vinylpyridine) (c-P2VP) *decrease* with decreasing molecular weight, although the difference in glass transition temperature (ΔT_g) between higher T_g cyclic samples and lower T_g linear samples with the same degree of polymerization progressively increases with decreasing molecular weight.[40]

As expected, the T_g values observed for a range of molecular weights of **c-PFS** with $M_n > 10\,000$ are comparable to the T_g recorded for high molecular weight samples of **l-PFS** (33−35 °C). As molecular weight decreases, T_g's measured for **c-PFS** decrease, while ΔT_g increases between **c-PFS** and **l-PFS** of similar molecular weights (Figure 3). Thus, cyclization has a similar effect on the glass temperature of **c-PFS** to that reported for samples of c-PS and c-P2VP.

2.3. Crystallization Behavior of c-PFS. As exothermic transitions corresponding to the melting of polymer crystallites (T_m) were observed in DSC traces of **c-PFS** (Figure S12), the crystallinity of these samples was further investigated by wide-angle X-ray scattering (WAXS) analysis. Linear PFSs which are symmetrically substituted at the bridging silicon (e.g., poly(ferrocenyldimethylsilane) **8**) will crystallize.[35,36] This crystallinity has been implicated in the unusual propensity of PFS-containing block copolymers to form cylindrical micelles in solutions of nonsolvents for the organometallic block.[41] WAXS analysis of **8** showed a strong reflection at a *d*-spacing of ∼6.28 Å. This distance was assigned to the spacing between planes of iron atoms in the polymer.[36,42] To confirm this assignment, the structure of the linear pentamer $\mathbf{5_5}$ was determined by single crystal X-ray diffraction. Using this diffraction data, a WAXS ($2\theta = 5°-50°$) pattern for the linear pentamer $\mathbf{5_5}$ was simulated and found to contain a strong reflection at $d = 6.28$ Å, which agreed with the *d*-spacing found in the corresponding high molecular weight polymer.[30]

To examine the influence of a cyclic topology on the morphological behavior of PFS, we compared experimental wide-angle X-ray scattering (WAXS) patterns collected for **c-PFS** with those for the semicrystalline linear PFS high molecular weight polymer prepared by anionic polymerization initiated with *n*BuLi (**8**). As single crystal X-ray structures of a range of low molecular weight cyclic oligomers $\mathbf{2_4}-\mathbf{2_7}$ were obtained (*vide infra*), experimental WAXS patterns were also compared with the strongest reflections observed in WAXS patterns simulated for $\mathbf{2_4}-\mathbf{2_7}$ using single-crystal diffraction data and the program PLATON[43] (see Supporting Information, Figure S6).

Samples of **l-PFS** and **c-PFS** were crystallized from THF/hexanes solvent mixtures (1:1; 25 °C, 48 h). The WAXS patterns collected for the high molecular weight polymer samples were virtually identical (compare e.g., (b) and (c) in Figure 4). This suggests that the lattice parameters in the samples are similar. Accordingly, the simulated diffractogram for the linear oligomer $\mathbf{5_5}$ exhibited features consistent with the patterns obtained for both linear and cyclic higher molecular weight polymer samples. Thus, $\mathbf{5_5}$ was confirmed to be an appropriate model for PFS high polymer, while, as expected, the conformations and crystal structures of the cyclic oligomers $\mathbf{2_{4-7}}$ cannot be said to appropriately model crystalline regions of cyclic high polymer based on the WAXS data.

(38) Clarson, S. J.; Dodgson, K.; Semlyen, J. A. *Polymer* **1985**, *26*, 930.
(39) Santangelo, P. G.; Roland, C. M.; Chang, T.; Cho, D.; Roovers, J. *Macromolecules* **2001**, *34*, 9002.
(40) Gan, Y.; Dong, D.; Hogen-Esch, T. E. *Macromolecules* **1995**, *28*, 383.
(41) (a) Massey, J. A.; Temple, K.; Cao, L.; Rharbi, Y.; Raez, J.; Winnik, M. A.; Manners, I. *J. Am. Chem. Soc.* **2000**, *122*, 11577. (b) Wang, X.; Guerin, G.; Wang, H.; Wang, Y.; Manners, I.; Winnik, M. A. *Science* **2007**, *317*, 644. (c) Gädt, T.; Ieong, N. S.; Cambridge, G.; Winnik, M. A.; Manners, I. *Nat. Mater.* **2009**, *8*, 144.
(42) (a) Barlow, S.; Rohl, A. L.; Shi, S.; Freeman, C. M.; O'Hare, D. *J. Am. Chem. Soc.* **1996**, *118*, 7578. (b) Rasburn, J.; Petersen, R.; Jahr, R.; Rulkens, R.; Manners, I.; Vancso, G. J. *Chem. Mater.* **1995**, *7*, 871.
(43) Spek, A. L. *J. Appl. Crystallogr.* **2003**, *36*, 7.

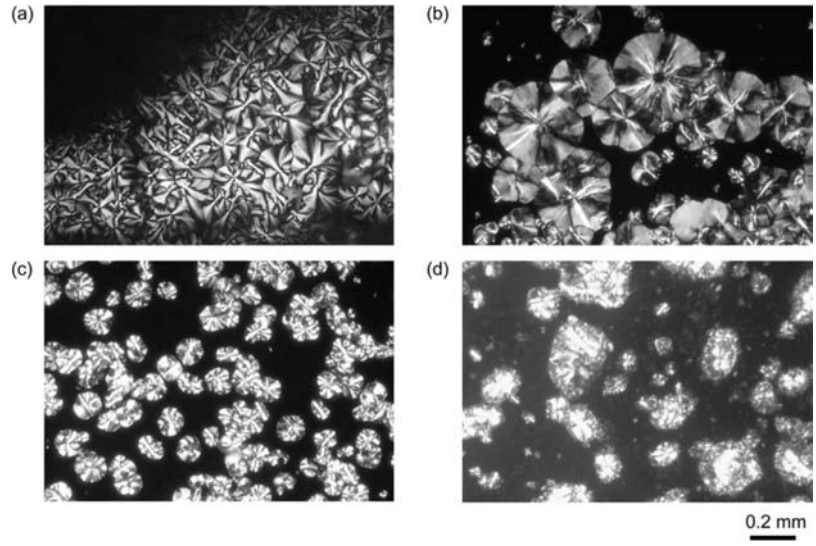

Figure 5. Polarizing optical micrographs of films of (a) **l-PFS**: M_n = 13 370, PDI = 1.15; (b) **l-PFS**: M_n = 6570, PDI = 1.06; (c) **c-PFS**: M_n = 12 750, PDI = 1.50; (d) **c-PFS**: M_n = 3990, PDI = 1.13. Samples were heated at 160 °C for 1 h and then cooled to 25 °C at 1 °C/min. Amorphous areas appear dark under cross-polars.

Interestingly, at lower molecular weights (~5000 Da) the crystalline structure of **l-PFS** produced diffraction peaks at values of 2θ that were not observed for either higher molecular weight **l-PFS** samples or low or high molecular weight **c-PFS** (compare (a) to (b) and (c) in Figure 4). This suggests that at lower molecular weights, the end groups in linear PFS influence chain packing. Indeed, it was observed that in the solid-state structures of $\mathbf{5_5}$ (and also the linear trimer, $\mathbf{5_3}$) the terminal ferrocenyl groups are twisted in opposite directions orthogonal to the interior ferrocenyl unit(s).[30]

To compare the spherulites formed in crystalline films of linear and cyclic PFS, samples were heated above the melting temperature to 160 °C, for 1 h, and then cooled at 1 °C/min and examined using a polarizing optical microscope. As expected from the similar diffraction patterns observed from WAXS experiments, applying cross-polar filters did not reveal any differences in appearance of the spherulites for the cyclic polymer sample compared to the linear sample (Figure 5). However, the size of spherulites of **l-PFS** were noticeably larger than those observed in cyclic samples. Spherulites of cyclic polytetrahydrofuran also appear smaller than those observed for analogous linear polymer samples.[44] In this case, negative birefringent spherulites with banded structures were observed for the cyclic polymer; however these were not observed for **c-PFS** in our experiments.

2.4. Physical Properties and X-ray Crystallographic Characterization of the Cyclic Oligo(ferrocenylsilanes) $\mathbf{2_{2-7}}$. The smallest cyclic oligo(ferrocenyldimethylsilanes) $\mathbf{2_{2-7}}$ were isolated as crystalline, air-stable, amber solids. The cyclic oligomers are readily soluble in aromatic and chlorinated solvents. Interestingly, $\mathbf{2_3}$ and $\mathbf{2_4}$ rapidly crystallize from such solvents and even more so from THF or diethyl ether. Like their linear counterparts,[30] the solubility of the oligomers in nonpolar solvents such as hexanes or pentane decreases with increasing ring size. Accordingly, separation of the cyclic oligo(ferrocenylsilanes) using a silica gel column was achieved using a gradient of 0−70% CH_2Cl_2 in hexanes. However, compounds $\mathbf{2_3}$ and $\mathbf{2_4}$ showed a tendency to crystallize and deposit on the column. Thus, while a majority of these compounds remained in solution and eluted in order of cycle size, a proportion of $\mathbf{2_3}$ and $\mathbf{2_4}$ eluted from the column only alongside higher molecular weight **c-PFS** with 100% CH_2Cl_2. The trimer and tetramer were then separated from the PFS fraction by crystallization from CH_2Cl_2 or THF and from one another using a subsequent column.

Table 4. Physical Properties of Cyclic and Linear Oligo(ferrocenylsilanes)

cyclic oligomer	δ (^{1}H)[a] C_5H_4	δ (^{1}H)[a] $SiMe_2$	R_F[b]	mp (°C)	linear oligomer[30]	R_F[b]	mp (°C)
$\mathbf{2_2}$	4.43, 4.35	0.31	0.37	235[17]	$\mathbf{5_2}$	0.39	97−98
$\mathbf{2_3}$	4.88, 4.50, 4.23	0.37	0.11	326[c]	$\mathbf{5_3}$	0.28	146
$\mathbf{2_4}$	4.27, 4.15	0.49	0.09	294[c]	$\mathbf{5_4}$	0.18	117−118
$\mathbf{2_5}$	4.25, 4.00	0.37	0.08	253−254	$\mathbf{5_5}$	0.13	172
$\mathbf{2_6}$	4.24, 4.05	0.44	0.04	200−201	$\mathbf{5_6}$	0.09	136−137
$\mathbf{2_7}$	4.24, 4.03	0.46	0.03	156	$\mathbf{5_7}$	0.07	146−147

[a] ppm; C_6D_6 (7.16 ppm). [b] Thin layer chromatography (TLC), silica gel, 15% dichloromethane in cyclohexane as eluent. [c] Decomposition.

The retention factors and melting points of solid cyclic oligomers $\mathbf{2_{2-7}}$ are presented alongside those of a previously reported series of linear oligo(ferrocenylsilanes) ($\mathbf{5_{2-7}}$) in Table 4. The cyclic oligomers (R_F = 0.03−0.37) are not retained to significantly greater extent on silica than the linear oligomers (R_F = 0.07−0.39). The melting points of cyclic oligomers are higher than those for the linear series, suggesting a greater lattice energy for the corresponding crystalline cycles. Unlike the linear series, the melting points decrease with increasing ring size, suggesting a high degree of crystallinity for the smaller cycles. This is particularly so in the case of $\mathbf{2_3}$ and $\mathbf{2_4}$ which decompose in air prior to melting at 326 and 294 °C, respectively.

The cycles $\mathbf{2_{4-7}}$ were characterized by ^{1}H, ^{13}C, and ^{29}Si NMR spectroscopy and, as expected, showed simple patterns with no signals for end groups. In all cases, only a single resonance was observed in the ^{29}Si NMR spectrum at approximately −6 ppm. In the ^{1}H NMR spectra, two pseudo triplet resonances were observed for the sets of Cp protons in positions α- and β- to the bridging silicon of $\mathbf{2_2}$ and $\mathbf{2_{4-7}}$. This is consistent with ^{1}H NMR spectra of PFSs in general, for which only two pseudo triplets for the Cp protons are typically observed. The ^{1}H NMR spectra of the trimeric $\mathbf{2_3}$, however, contained three broad

(44) Tezuka, Y.; Ohtsuka, T.; Adachi, K.; Komiya, R.; Ohno, N.; Okui, N. *Macromol. Rapid Commun.* **2008**, *29*, 1237.

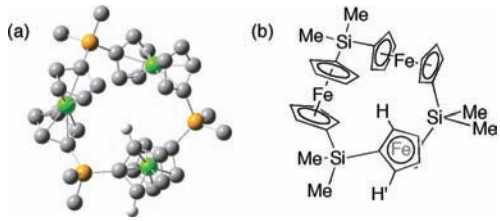

Figure 6. (a) Calculated structure of $\mathbf{2_3}$. For clarity, only one set of protons, α to a bridging $SiMe_2$, are shown. (b) Diagram illustrating two distinct magnetic environments for protons adjacent the $SiMe_2$ bridge: H and H′. Above 55 °C, these environments interchange on the NMR time scale.

singlets in the aromatic region, with integrations corresponding to a proton ratio of 1:2:1 at room temperature.

To better understand the ^{1}H NMR spectrum of $\mathbf{2_3}$, the structure of $\mathbf{2_3}$ was calculated by DFT methods.[45] In the optimized structure (Figure 6), one set of Cp hydrogen atoms adjacent to the bridging silicon point toward the center of the cyclic oligomer, while the $SiMe_2$ and the second set of hydrogens are oriented *exo* to the macrocyclic ring. The three ^{1}H NMR spectroscopic resonances observed for each cyclopentadienyl ring may be explained by preferential shielding of one set of proton nuclei α- to the bridging silicon. Thus, in the ^{1}H NMR spectrum (in $CDCl_3$), two signals are observed for the α-H's in a 1:1 ratio at 4.88 and 4.23 ppm, while the third signal which integrated to two protons corresponds to the proton nuclei *β*- to the silicon spacer (4.50 ppm).

At −90 °C, the peaks are not further resolved. Above 55 °C, the two resonances assigned to the α-protons coalesced, indicating that the two sets of α-protons have become equivalent on the NMR time scale. In the ^{13}C{^{1}H} NMR spectrum (25 °C), all five Cp carbon nuclei are inequivalent and five signals were observed in the aromatic region. In addition, only a single resonance was detected by ^{29}Si DEPT NMR spectroscopy (−6.4 ppm).

As mentioned above, the solid-state structures of $\mathbf{2_{4-7}}$ were determined by single crystal X-ray diffraction (Figures 7 and 8). The structure of the cyclic dimer $\mathbf{2_2}$ has been previously reported.[17] The Fe−C and Si−C bond distances in $\mathbf{2_{4-7}}$ are similar to those of the previously reported linear oligomers $\mathbf{5_3}$ and $\mathbf{5_5}$. Tetragonal symmetry renders all intramolecular Fe−Fe distances between adjacent ferrocene units in $\mathbf{2_4}$ equivalent at a compact value: 5.5659(9) Å. The intramolecular Fe−Fe distances in $\mathbf{2_5}$ range from 5.9038(7) Å [*d*(Fe(1)−Fe(2)] to 6.3426(7) Å [*d*(Fe(5)−Fe(1)], and the corresponding distances in $\mathbf{2_6}$ range from 5.640(2) Å [*d*(Fe(2)−Fe(3)] to 6.107(2) Å [*d*(Fe(1)−Fe(2)]. All Fe−Fe distances in $\mathbf{2_7}$ are different and

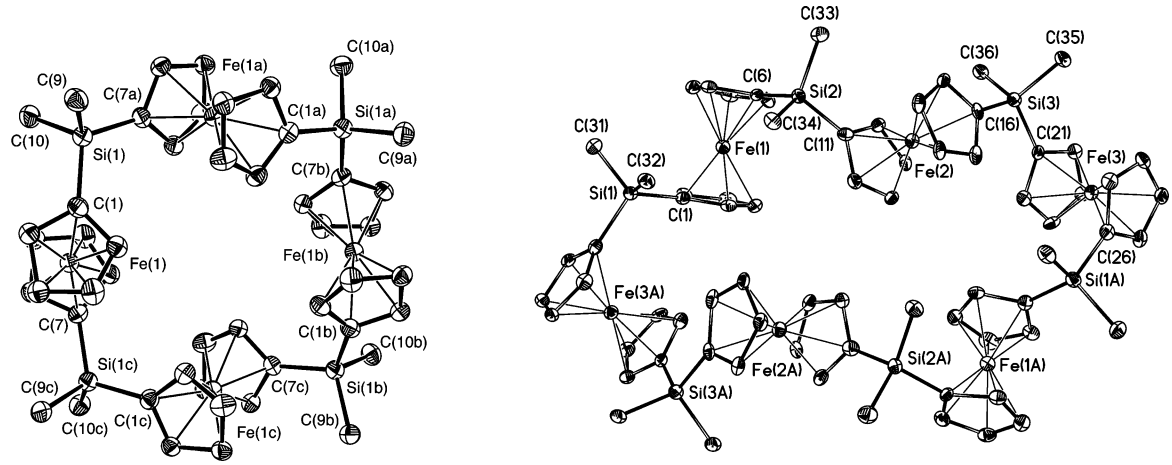

Figure 7. Solid-state structures of cyclic oligomers with an even number of ferrocene units: $\mathbf{2_4}$ and $\mathbf{2_6}$. Thermal ellipsoids are shown at 30% probability.

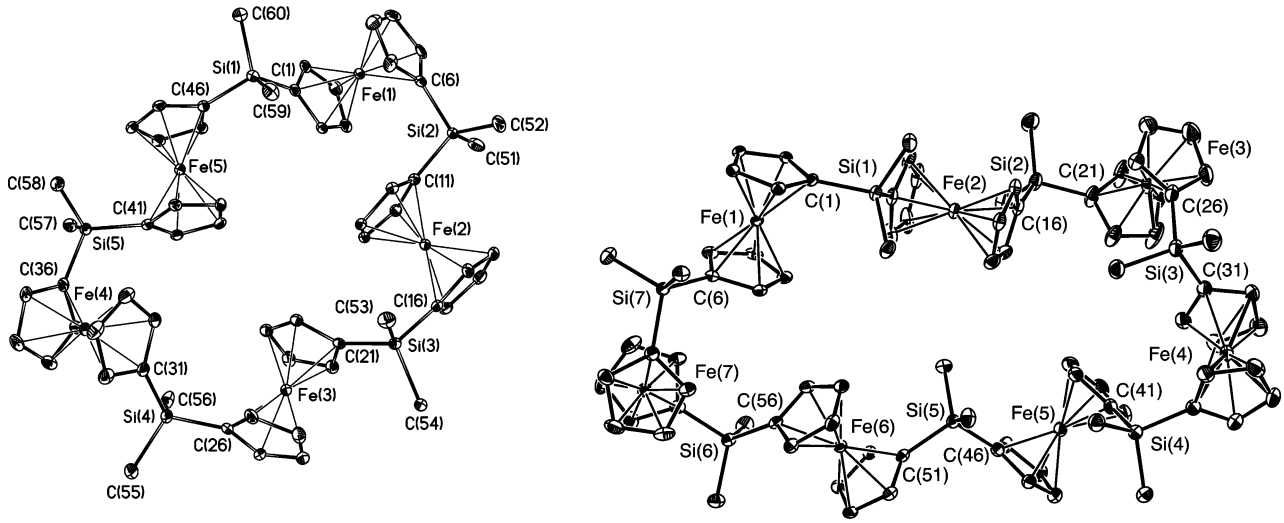

Figure 8. Solid-state structures of cyclic oligomers with an odd number of ferrocene units: $\mathbf{2_5}$ and $\mathbf{2_7}$. Thermal ellipsoids are shown at 30% probability.

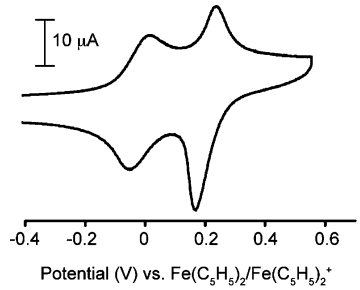

Figure 9. Cyclic voltammogram of **c-PFS** (M_n = 12 370) in 50:50 PhCN/CH_2Cl_2. Analyte concentration was 1.9×10^{-3} M in terms of the monomer unit and 0.1 M in the supporting electrolyte $[Bu_4N][PF_6]$. The scan rate was 200 mV/s.

show the largest variation from 5.9369(6) Å [*d*(Fe(7)−Fe(1)] to 6.9887(7) Å [*d*(Fe(5)−Fe(6)].

In comparison, intramolecular distances between neighboring iron atoms in $\mathbf{5_3}$ and $\mathbf{5_5}$ are longer than those for the smaller cycles (6.187(4) Å and 6.056(5) to 6.913(5) Å, respectively).[29,30] Only the larger seven-unit $\mathbf{2_7}$ has comparable iron−iron separations to the linear pentamer. The iron−iron distances in the cyclic oligomers are shorter due to their constrained ring structures. The relaxation of these distances with increasing ring size is reflected in the observed electrochemical behavior of $\mathbf{2_2}$-$\mathbf{2_4}$ compared to $\mathbf{2_5}$-$\mathbf{2_7}$, as discussed in the following section.

2.5. Electrochemical Studies of Cyclic Oligo- and Polyferrocenylsilanes. Polymers containing redox-active metals in their main chains are increasingly of interest as stimuli-responsive soft materials for device fabrication and ion sensing.[12,46] **l-PFSs**, for example, show electronic communication between adjacent ferrocene units which results in a two-wave pattern in cyclic voltammograms (CVs) of PFSs.[47] This electroactivity has been exploited to make capsules with redox-controlled permeation,[48] responsive mechanical systems,[49] and photonic crystal devices.[50] We found that the characteristic two-wave pattern noted for linear analogues was reproduced in CVs of **c-PFSs** (Figure 9, Table 5). Oxidation peaks occurred at the same potential, regardless of the molecular weight of the sample. The sharp feature (180 mV cathodic potential) can be attributed to plating of oxidized PFS on the electrode upon oxidation, perturbing the rate of diffusion at the electrode.

Linear oligoferrocenyldimethylsilanes have been previously studied and were shown to exhibit similar electronic communication between adjacent metal centers.[30,51] These were used as electrochemical models to explain the aforementioned two-wave redox behavior observed for **l-PFS** high molecular weight polymers: initial oxidation occurs at alternating iron centers, with oxidation of the intervening ferrocene sites at a higher potential.[30,52] To explore how the configuration of redox centers in a cyclic structure affects electronic communication, we also investigated the electrochemical behavior of cyclic oligoferrocenylsilanes $\mathbf{2_2}$−$\mathbf{2_7}$. The electrochemical behavior of $\mathbf{2_2}$−$\mathbf{2_7}$ was examined by CV and differential pulse voltammetry (DPV). We first attempted experiments in CH_2Cl_2 and then a solvent mixture of 1:1 CH_2Cl_2/CH_3CN, which was found previously to be compatible with both neutral and oxidized linear PFS oligomers.[30] In both cases, however, we observed substantial deposition of the oligoferroceniumsilanes onto the electrode surfaces. This was remedied by employing a 1:1 mixture of C_6H_5CN/CH_2Cl_2. and the results are given in Figures 10 and 11 and Table 6. DPVs can be found in the Supporting Information (Figures S8−S10).

Table 5. Electrochemical Data for **c-PFS**[a]

M_n[b]	$E^1_{1/2}$	$E^2_{1/2}$	$E^2_{1/2}-E^1_{1/2}$
12 370	−0.02	0.21	0.23
26 310	−0.02	0.21	0.23

[a] Peak potentials obtained from differential pulse voltammograms. All values in V vs $Fe(C_5H_5)_2/Fe(C_5H_5)_2^+$. [b] Determined by GPC (triple detection).

The cyclic dimer $\mathbf{2_2}$ produced an unambiguous voltammogram showing two waves of equal height, separated by 0.24 V, suggesting two one-electron oxidations from strongly interacting iron centers (Scheme 3a).[17] The tetramer, $\mathbf{2_4}$, showed two broad peaks, indicative of two sets of two overlapping one-electron processes (Scheme 3c). This is consistent with a compact molecule in which short intramolecular iron−iron separations cause Coulombic repulsion between ferrocenium units.[53] Whereas, the hexamer $\mathbf{2_6}$ exhibited two even broader peaks in an approximate 1:1 ratio, in which initial oxidation at alternating ferrocene units is followed by oxidation at the intervening iron centers at higher potential (Scheme 3e). In comparison, Astruc and co-workers have reported the synthesis and electrochemical behavior of hexakis(ferrocenylethynyl)benzene (**10**), which contains six ferrocene units assembled around a rigid conjugated platform.[54] In CH_2Cl_2, using $[Bu_4N][PF_6]$ as the supporting electrolyte, no significant communication between iron centers through the polyethynylbenzene core was observed and oxidation of all six ferrocene units occurred at the same potential.

Unlike the "odd-numbered" linear oligomers $\mathbf{5_x}$,[30] a three-wave pattern of reversible oxidation processes is expected from CVs of cyclic oligomers with an odd number of ferrocene units. For $\mathbf{2_3}$, $\mathbf{2_5}$, and $\mathbf{2_7}$, this resulted in three-wave patterns where the first and last waves are of equal intensity and the ratio of these to the middle wave increases with increasing ring size (Figure 11). For example, three one-electron oxidations of approximately the same size are observed for the trimer $\mathbf{2_3}$ and are well-resolved as a result of the compact ring size (Scheme 3b). The CV of the cyclic pentamer $\mathbf{2_5}$ shows reversible oxidation processes in an approximate 2:1:2 ratio (Scheme 3d). For $\mathbf{2_7}$, a 3:1:3 pattern was expected (Scheme 3f). The middle redox event, however, was not well resolved, in contrast to

(45) The cyclic trimer $\mathbf{2_3}$ rapidly crystallized under a number of experimental conditions as very small bunches of needles. While a partial structure was obtained using Cu radiation and connectivity of the trimer was confirmed, single crystals could not be grown large enough for a complete X-ray diffraction structure determination.
(46) (a) Casado, C. M.; Cuadrado, I.; Morán, M.; Alonso, B.; García, B.; González, B.; Losada, J. *Coord. Chem. Rev.* **1999**, *185*, 53. (b) Armada, M. P. G.; Losada, J.; Zamora, M.; Alonso, B.; Cuadrado, I.; Casado, C. M. *Bioelectrochem.* **2006**, *69*, 65. (c) Ornelas, C.; Ruiz, J.; Belin, C.; Astruc, D. *J. Am. Chem. Soc.* **2009**, *131*, 590.
(47) Foucher, D. A.; Honeyman, C. H.; Nelson, J. M.; Tang, B. Z.; Manners, I. *Angew. Chem. Int. Ed. Engl.* **1993**, *32*, 1709.
(48) Ma, Y.; Dong, W.-F.; Hempenius, M. A.; Moehwald, H.; Vancso, G. J. *Nat. Mater.* **2006**, *5*, 724.
(49) (a) Shi, W.; Giannotti, M. I.; Zhang, X.; Hempenius, M. A.; Schönherr, H.; Vancso, G. J. *Angew. Chem. Int. Ed.* **2007**, *46*, 8400. (b) Hempenius, M. A.; Cirmi, C.; Song, J.; Vancso, G. J. *Macromolecules* **2009**, *42*, 2324.
(50) Arsenault, A. C.; Puzzo, D. P.; Manners, I.; Ozin, G. A. *Nat. Photonics* **2007**, *1*, 468.
(51) For related work on oligoferrocenes, see: Hirao, T.; Kurashina, M.; Aramaki, K.; Nishihara, H. *J. Chem. Soc., Dalton Trans.* **1996**, 2929.
(52) Aoki, K.; Chen, J. *J. Electroanal. Chem.* **1995**, *380*, 35.
(53) Aoki, K. *J. Electroanal. Chem.* **1995**, *381*, 185.
(54) Diallo, A. K.; Daran, J.-C.; Varret, F.; Ruiz, J.; Astruc, D. *Angew. Chem. Int. Ed.* **2009**, *48*, 3141.

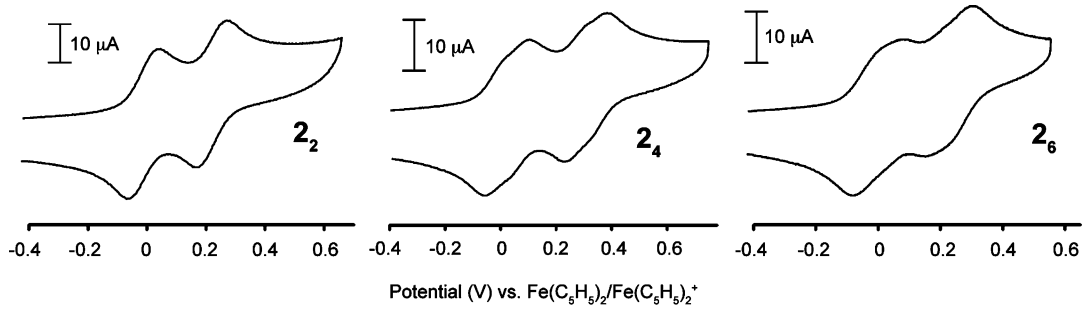

Figure 10. Cyclic voltammograms of cyclic oligoferrocenylsilanes with an even number of ferrocene units. CVs were performed in 1:1 CH_2Cl_2/C_6H_5CN solutions at scan rates of 200 mV/s with 0.1 M $[Bu_4N][PF_6]$. The concentrations of analyte were 7.8×10^{-4}, 7.4×10^{-4}, and 3.4×10^{-4} M for $\mathbf{2_2}$, $\mathbf{2_4}$, and $\mathbf{2_6}$, respectively.

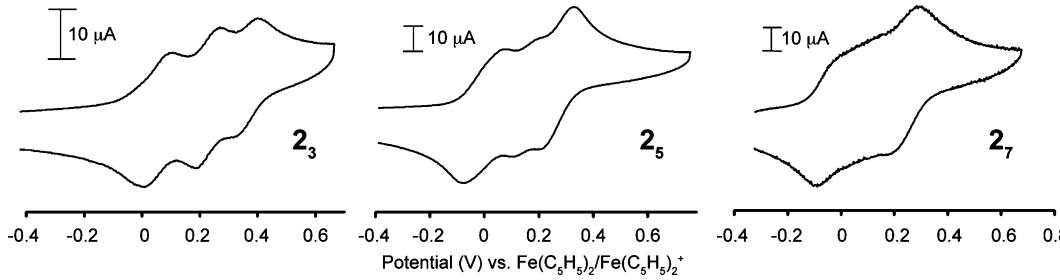

Figure 11. Cyclic voltammograms of cyclic oligoferrocenylsilanes with an odd number of ferrocene units. With the exception of $\mathbf{2_7}$ (1:1 CH_2Cl_2/CH_3CN), all CVs were performed in 1:1 CH_2Cl_2/C_6H_5CN solutions at scan rates of 200 mV/s with 0.1 M $[Bu_4N][PF_6]$. The concentrations of analyte were 6.6×10^{-4}, 1.2×10^{-3}, and 6.8×10^{-4} M for $\mathbf{2_3}$, $\mathbf{2_5}$, and $\mathbf{2_7}$, respectively.

Table 6. Electrochemical Data for Cyclic Oligo(ferrocenyldimethylsilane)s $\mathbf{2_2}-\mathbf{2_7}$[a]

oligomer	$E^1_{1/2}$	$E^2_{1/2}$	$E^3_{1/2}$	$E^4_{1/2}$	$E^2_{1/2}-E^1_{1/2}$	$E^3_{1/2}-E^2_{1/2}$
$\mathbf{2_2}$	−0.01 (1e⁻)	0.23 (1e⁻)	−	−	0.24	−
$\mathbf{2_3}$	0.03 (1e⁻)	0.21 (1e⁻)	0.34 (1e⁻)	−	0.18	0.13
$\mathbf{2_4}$	0.02 (2e⁻)	*b*	0.30 (2e⁻)	*b*	0.28	−
$\mathbf{2_5}$	−0.02 (2e⁻)	0.15 (1e⁻)	0.25(2e⁻)	−	0.17	0.10
$\mathbf{2_6}$	−0.01 (3e⁻)	0.23 (3e⁻)	−	−	0.24	−
$\mathbf{2_7}$	−0.01 (3e⁻)	*b*	0.24 (4e⁻)	−	*b*	0.25

[a] Peak potentials obtained from differential pulse voltammograms (see Figures S8−S10). Symbolism: $E^n_{1/2}$ (ne^-): potential of *m*th wave having stoichiometry of *n* electrons. All values in V vs $Fe(C_5H_5)_2/Fe(C_5H_5)_2^+$. [b] Peak was not resolved.

Scheme 3. A Graphical Representation of the Electrochemical Behavior of the Series of Cyclic Oligomers[a]

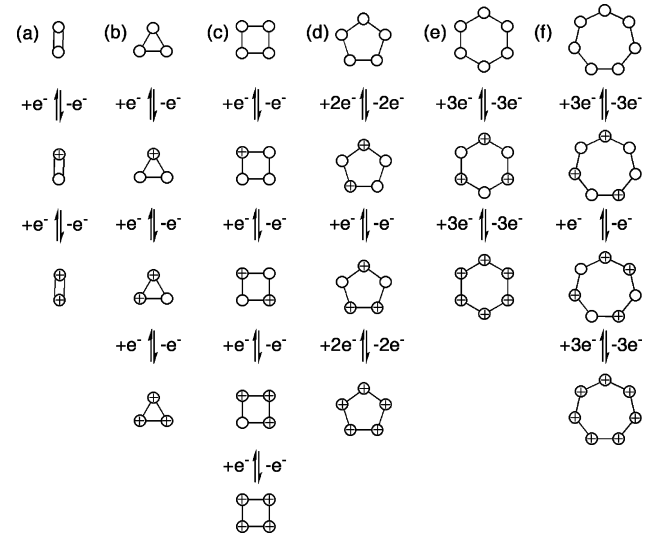

[a] (a) $\mathbf{2_2}$, (b) $\mathbf{2_3}$, (c) $\mathbf{2_4}$, (d) $\mathbf{2_5}$, (e) $\mathbf{2_6}$, (f) $\mathbf{2_7}$. Each circle represents a ferrocene unit.

Köhler's more soluble cyclic heptamer (**3**) in which the three expected chemically reversible waves were detected.[21]

These results suggest that Coulombic interactions[55] dictate the stepwise oxidation of the macrocycles and the effect of an adjacent positive charge is more strongly felt in the small, more constrained cycles $\mathbf{2_3}$ and $\mathbf{2_4}$ consistent with strong through-space interactions. The potential separation between the first and last oxidation waves for $\mathbf{2_2}$, $\mathbf{2_5}$, $\mathbf{2_6}$, and $\mathbf{2_7}$ is essentially constant (0.23−0.24 V). This value is 0.31 V for $\mathbf{2_3}$ and 0.28 V for $\mathbf{2_4}$. The increase in the spread of $E_{1/2}$ values arises from the close proximity of ferrocenium groups next to the remaining iron centers following the initial oxidation processes.

In contrast, the reversible redox processes observed for the previously reported series of linear oligomers ($\mathbf{5}_x$) are, in a sense, the opposite of those observed for $\mathbf{2}_{2-7}$. For $\mathbf{5}_x$, three reversible redox processes of varying intensity were observed for the linear oligomers containing an *even* number of ferrocene units, while two-wave patterns were observed for *odd* numbered oligomers.[30] Constraining the oligomers into cyclic structures causes significant differences to the observed electrochemistry: two-wave redox patterns are observed for cyclic oligomers with an even

(55) The role of the spacer group in mediating these interactions appears to involve two effects: (i) the size of the spacer influences the metal−metal separation and (ii) the polarizability of the spacer influences the dielectric constant of the medium between the metal centers. Strong interactions are therefore promoted by small, highly polarizable spacers. See: (a) Dement'ev, V. V.; Cervantes-Lee, F.; Parkanyi, L.; Sharma, H.; Pannell, K. H.; Nguyen, M. T.; Diaz, A. *Organometallics* **1993**, *12*, 1983. (b) Deck, P. A.; Lane, M. J.; Montgomery, J. L.; Slebodnick, C.; Fronczek, F. R. *Organometallics* **2000**, *19*, 1013. (c) Southard, G. E.; Curtis, M. D. *Organometallics* **2001**, *20*, 508. (d) Barriere, F.; Camire, N.; Geiger, W. E.; Mueller-Westerhoff, U. T.; Sanders, R. *J. Am. Chem. Soc.* **2002**, *124*, 7262. (e) Kaufmann, L.; Breunig, J.-M.; Vitze, H.; Schoedel, F.; Nowik, I.; Pichlmaier, M.; Bolte, M.; Lerner, H.-W.; Winter, R. F.; Herber, R. H.; Wagner, M. *Dalton Trans.* **2009**, 2940.

number of ferrocene units, while those with an odd number of ferrocene moieties produced an odd number of waves (unresolved in $\mathbf{2_7}$).

3. Summary and Conclusions

A convenient method for the preparation of redox-active **c-PFS** is reported. Conversion of monomer to cyclic polymer and the ratio of smaller oligomers to polymer were found to depend on the concentration, reaction temperature, and irradiation time. This allowed access to **c-PFSs** with a range of molecular weights. MALDI-TOF mass spectrometry and NMR spectroscopy were used to establish the absence of end groups for the cyclic macromolecules of moderate molecular weights. **c-PFSs** showed a more compact structure in solution than **l-PFSs** of similar molecular weight, and smaller hydrodynamic radii and lower solution viscosity were measured for cyclic samples. Our proposed mechanism of macrocycle formation does not rule out the presence of linear PFS contaminants which could result in threading of **c-PFS** rings and other more complex topologies. However, GPC traces of crude **c-PFS** samples showed no tailing into the higher molecular region, consistent with the predominance of backbiting intramolecular cyclization reactions over intermolecular macrocondensation.

DSC, WAXS, and polarizing optical microscopy studies were utilized to establish the crystallinity of **c-PFS**. The WAXS patterns of low-molecular weight **c-PFS** samples were comparable to those observed for high, rather than low, molecular weight **l-PFS**, indicating the prominent effect of end groups on the morphological behavior of the latter. Additionally, **c-PFS** with smaller values of M_n underwent the glass transition at significantly higher temperatures than corresponding samples of **l-PFS**, consistent with the decreased mobility of the cyclic polymer chains which lack end groups.

Cyclic oligomers $\mathbf{2_3}-\mathbf{2_7}$ were isolated by column chromatography and fully characterized. The solid-state structures of these oligomers helped to explain their observed electrochemical behavior. For example, the close proximity of ferrocene units in the tetramer $\mathbf{2_4}$ increased the spread of $E_{1/2}$ potentials at which the first and last redox event occurred relative to higher cyclic oligomers with greater intramolecular iron−iron separation, and hence less Coulombic interaction. A similarly large potential separation was observed due to the compact structure of cyclic trimer $\mathbf{2_3}$.

Photocontrolled ring-opening oligomerization and polymerization using substitutionally labile Lewis bases as initiators therefore offer opportunities to access **c-PFSs** with different molecular weights. This protocol is likely applicable to other strained metal-containing rings, potentially including analogous monomers composed of different metals, π-hydrocarbon ligands, and bridging groups.[14]

Acknowledgment. We thank the EPSRC for support, the European Union for a Marie Curie Chair, and the Royal Society for a Wolfson Research Merit Award (I.M.). D.E.H., W.Y.C., and J.B.G. thank the Natural Sciences and Engineering Research Council of Canada for financial support. We thank Prof. Neil G. Connelly for the use of electrochemical equipment and Dr. Charl Faul for the use of a polarizing optical microscope.

Supporting Information Available: (1) Experimental and computational methods and details, (2) Simulated WAXS patterns for $\mathbf{2_4}$-$\mathbf{2_7}$, (3) DPV results for $\mathbf{2_2}-\mathbf{2_7}$, (4) DSC traces of **c-PFSs**. This material is available free of charge via the Internet at http://pubs.acs.org.

JA904928C